

# Single-Frequency Nd:YVO<sub>4</sub> Laser at 671 nm With High-Output Power of 2.8 W

Yaohui Zheng, Yajun Wang, Changde Xie, and Kunchi Peng

**Abstract**—A high-power single-frequency laser at 671 and 1342 nm is designed and built. We find that for a high power Nd:YVO<sub>4</sub> laser, the thermal load of gain medium at 1342 nm lasing is much more stronger than that without lasing, which results in a bistability-like phenomenon on the relation curve between the output power and pump power. Based on the consideration to this special phenomenon, in our design, the cavity parameters are optimized carefully to satisfy the laser stability condition for both cases before and after lasing, the thermal effect of the Nd:YVO<sub>4</sub> crystal is mitigated by increasing appropriately the fundamental mode size. The maximal output powers of 2.8 W at 671 nm and 850 mW at 1342 nm are simultaneously achieved.

**Index Terms**—Optical harmonic generation, ring optical resonator, solid-state lasers, thermal effect.

## I. INTRODUCTION

SINGLE-FREQUENCY Nd:YVO<sub>4</sub> lasers operating in the 1.3- $\mu\text{m}$  spectral region are desirable for their potentially important applications in medical diagnosis, fiber optics and so on [1, 2]. The frequency-doubling laser of 1.3  $\mu\text{m}$  at 0.67  $\mu\text{m}$  can be used for high-precision laser spectroscopy and laser cooling of the Lithium (Li) atom [3]. Especially, in the field of quantum optics, it has been demonstrated that multicolored entanglement can be generated between the fundamental and second-harmonic fields based on a second-order nonlinear interaction [4, 5]. Due to that the 0.67  $\mu\text{m}$  laser is at the absorption line of Li atoms [6] and the 1.3  $\mu\text{m}$  laser is at a communication window of optical fibers, the two-color entangled beams are very useful in developing quantum information technology, where the Li atoms are used to the quantum memory and the optical fibers are used to the transmitting line of quantum information [7]. For preparing the entangled optical beams of 0.67  $\mu\text{m}$  and 1.3  $\mu\text{m}$  via a nonlinear interaction [4, 5], we have to construct a single-frequency CW laser with high-output power at the two wavelengths to be the pump field and the injected signal of an optical parametric amplifier (OPA), respectively.

Manuscript received July 25, 2011; revised November 15, 2011; accepted November 28, 2011. Date of current version December 20, 2011. This work was supported in part by the National Natural Science Foundation of China under Grant 61008001 and Grant 60736040, the National Basic Research of China under Program 2010CB923101, and the National High-Tech Research and Development of China under Program 2011AA030203.

The authors are with the State Key Laboratory of Quantum Optics and Quantum Optics Devices, Institute of Opto-Electronics, Shanxi University, Shanxi 030006, China (e-mail: yzheng@sxu.edu.cn; wangyajun\_166@163.com; changde@sxu.edu.cn; kcpeng@sxu.edu.cn).

Color versions of one or more of the figures in this paper are available online at <http://ieeexplore.ieee.org>.

Digital Object Identifier 10.1109/JQE.2011.2178398

Nd:YVO<sub>4</sub> lasers at 1.34  $\mu\text{m}$  and its second-harmonic red lasers have been extensively studied [8]–[11], and the maximal 9.9 W single-transverse red light output at 671 nm has been produced by a laser with a standing-wave resonator [10]. As well-known, it is difficult to operate a high-power laser at a stable single-frequency, so only the maximal single-frequency output of 370 mW at 671 nm was accomplished by an intracavity frequency-doubling Nd:YVO<sub>4</sub> laser with a standing-wave resonator [9]. Generally, the spatial hole burning of a laser crystal in a standing-wave laser limits its high-power single-frequency operation. In order to increase the output power and improve the stability of the single axial mode, usually the unidirectional ring cavity configuration is selected. Multi-watt single-frequency Nd:YVO<sub>4</sub> laser output at 532 nm has been achieved by using a unidirectional ring laser [12]. Recently, Camargo et al. reported a single-frequency Nd:YVO<sub>4</sub> laser with the maximal output power of 680 mW at 671 nm in which a ring resonator is also utilized [13]. However, comparing with the  ${}^4\text{F}_{3/2}$ – ${}^4\text{I}_{11/2}$  transition for 1064 nm, the  ${}^4\text{F}_{3/2}$ – ${}^4\text{I}_{13/2}$  transition for 1342 nm has weaker emission cross section, larger quantum energy defect, and excited-state absorption (ESA) [14–16], which still prevent from obtaining the multi-watt single-frequency red laser up to now.

In this paper, we present a multi-watt single-frequency red laser with a figure “8” shape ring cavity to be the axial mode selector and the LBO crystal to be the intracavity frequency-doubler. In the process of designing the laser we find that the Nd:YVO<sub>4</sub> crystal has unusually thermal characteristic for operating at 1342 nm comparing with operating at 1064 nm, namely, its thermal load at 1342 nm lasing is much more stronger than that without lasing. The thermal characteristic of Nd:YVO<sub>4</sub> crystal results in a bistability-like phenomenon on the relation curve between the output power and pump power. In addition, only when the stable condition is satisfied simultaneously at both cases with and without lasing, the laser can start to oscillate stably at 1342 nm. Based on the consideration to this special phenomenon, in our design, the cavity parameters are optimized carefully to satisfy the stable condition and increase appropriately the fundamental mode size. The maximal single-frequency output powers of 2.8 W at 671 nm and 850 mW at 1342 nm are simultaneously obtained under the pump power of 23.5 W. The mode-hop-free single-frequency operation of more than 3 h is observed. To the best of our knowledge, this is the largest single-frequency output power obtained for the 671 nm laser so far.

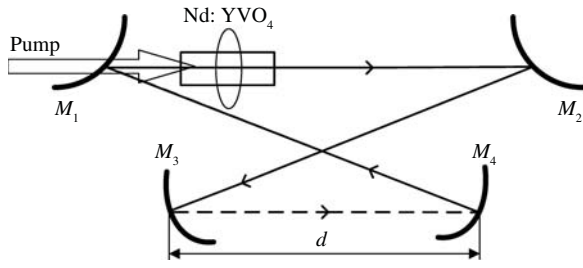


Fig. 1. Configuration of the laser resonator.

## II. DESIGN OF LASER RESONATOR

The main challenge to obtain high-power laser at 671 nm results from the strongly thermal effects of Nd:YVO<sub>4</sub> crystal at the wavelength of 1342 nm. In order to quantify the influence of the thermal effects on the laser operation at 1342 nm and find an optimal resonator configuration, we calculate the thermal focal length of Nd:YVO<sub>4</sub> crystal pumped directly by a laser diode (LD) at 880 nm [17–19]. The thermal focal length of the gain medium in an end-pumped laser can be expressed by [20]:

$$f_{th} = \frac{\pi K_c \omega_p^2}{\zeta_0 P (dn/dt) [1 - \exp(-\alpha l)]} \quad (1)$$

where  $K_c$  is the thermal conductivity (0.0523 W/cm/K),  $\omega_p$  is the pump beam radius (450  $\mu$ m),  $P$  is the incident pump power (23.5 W),  $dn/dt$  is the thermal-optic coefficient ( $2.9 \times 10^{-6}$ /K),  $\alpha$  is the absorption coefficient ( $1.5 \text{ cm}^{-1}$  for the Nd:YVO<sub>4</sub> crystal with doping concentration of 0.3%),  $l$  is the length of the gain medium (15 mm), and  $\zeta_0$  is the fractional thermal load (a fraction of the incident power deposited as heat). Assuming that all the parameters in Eq. (1), with an exception of  $\zeta_0$ , are invariable under conditions of both lasing and nonlasing, the thermal focal length is inversely proportional to the fractional thermal load  $\zeta_0$ , which depends on the laser action and the operating wavelength.

In Nd:YVO<sub>4</sub> lasers, the thermal load of an Nd:YVO<sub>4</sub> laser without lasing is mainly determined by the average fluorescence line and the pump wavelength [16], and is independent of the lasing wavelength. The fractional thermal load  $\zeta_0$  is approximately 22.5% of the pump power for 880 nm pumping before lasing (below the oscillation threshold of the laser) [21]. In Nd:YVO<sub>4</sub> lasers operating at 1064 nm, the thermal load is mainly related to the pump wavelength, and equals approximately 17.3% of the pumping power [21], when the wavelength of LD is 880 nm. The thermal load after lasing (above the threshold) at 1064 nm is slightly weaker than that of the laser below the threshold resulting from the effects of the multiphonon decay and various interionic upconversion processes [22, 23]. However, for Nd:YVO<sub>4</sub> lasers operating at 1342 nm, the thermal effect of the laser crystal is different from that operating at 1064 nm. The fractional thermal load  $\zeta_0$  at 1342 nm with lasing is mainly related to the strong excited state absorption (ESA) and quantum defect determined by both pump and laser wavelengths, and is approximately 41% for the laser pumped by LD at 880 nm [16] which is much larger than that before lasing ( $\sim 22.5\%$ ). From the parameters described

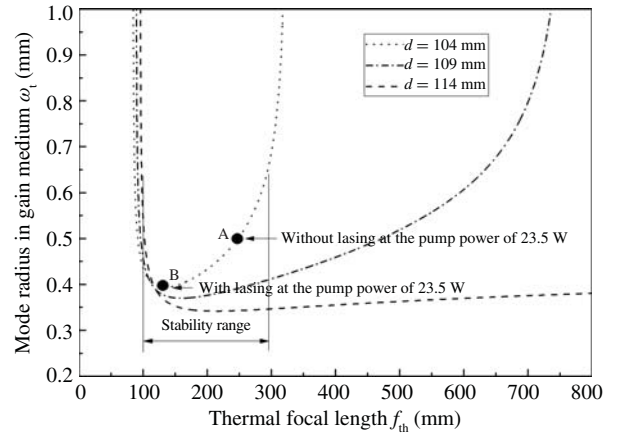


Fig. 2. Beam radius of fundamental wave in gain medium versus thermal focal length  $f_{th}$  for three different distances  $d$  between  $M_3$  and  $M_4$ .

above, we conclude that the thermal focal lengths before and after lasing at 1342 nm are about 242 mm and 133 mm, respectively, at the incident pump power of 23.5 W. With the increasing of pump power, the thermal focal length produces a steep change suddenly at the threshold power, due to the obvious difference of the thermal focus at the cases before and after lasing. The corresponding mode radius of the laser in the gain medium decreases instantly (Fig. 2). Hence, we have to consider the special characteristic, which is totally different from the 1064 nm laser in the 1342 nm laser design. We find, only when the stable condition is satisfied simultaneously at both cases before and after lasing, the laser can start to oscillate stably at 1342 nm.

In order to analyze the stable range of the resonator, we calculate the mode size in the gain medium as a function of the thermal focal length  $f_{th}$ , by means of the ABCD matrix under the approximation of a thin lens in the middle of the laser crystal.

The configuration of the laser resonator is shown in Fig. 1. The resonator consists of two convex mirrors ( $M_1$  and  $M_2$ ) and two concave mirrors ( $M_3$  and  $M_4$ ) [24]. The curvature radius of both  $M_3$  and  $M_4$  is fixed at 100 mm and the curvature radius of  $M_1$  and  $M_2$  is 1500 mm. The length of the laser path outside  $M_3$  and  $M_4$  ( $M_1 \rightarrow M_2 + M_2 \rightarrow M_3 + M_4 \rightarrow M_1$ ) is kept at 430 mm and is unchanged at all cases. Under three different distances ( $d$ ) between  $M_3$  and  $M_4$  (114 mm, 109 mm, and 104 mm), the function of the mode radii in the gain medium versus thermal focal lengths  $f_{th}$  are shown in Fig. 2. It can be seen that, when  $d$  equals 114 mm or 109 mm, the stable range is much larger than that of  $d = 104$  mm. However, the mode sizes for  $d = 104$  mm are larger than that of  $d = 114$  mm and 109 mm inside their stable ranges, thus the thermal effect of the gain medium with  $d = 104$  mm is less than that with  $d = 114$  mm and 109 mm [25]. More importantly, both operating points before (point A) and after (point B) lasing at the pump power of 23.5 W is included in the stable range of the resonator. In addition, the point B is at the center of the stable region, which is advantageous to the stable operation of the laser. If the distance  $d$  is shortened further, the resonator provides a much smaller stable range, which cannot

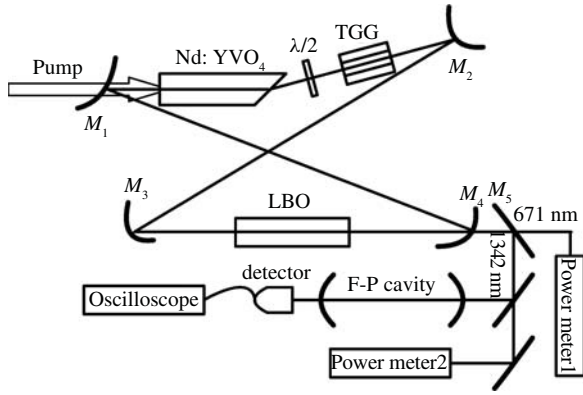


Fig. 3. Experimental schematic of the high-power single-frequency red laser.  $\lambda/2$ : half wave plate. TGG: terbium gallium garnet.

ensure that the two stable conditions before and after lasing are satisfied simultaneously. If  $d < 104$  mm, although the mode size possibly further increases, the two working points A and B will be out of the stable range. As a compromise, we take  $d = 104$  mm to reach a larger mode size and an appropriately stable range.

### III. EXPERIMENTAL ARRANGEMENT

The experimental setup is shown in Fig. 3. The pump source of the laser is a commercially available fiber-coupled diode array (JOLD-30-FC-14), which is partially polarized light. The peak emission wavelength of the pump light is temperature-tuned to the absorption line of Nd:YVO<sub>4</sub> crystal at 880 nm. The coupling fiber has a core diameter of 400  $\mu\text{m}$  and a numerical aperture (NA) of 0.22. The output of the fiber is focused by a focusing system, which consists of two lenses with focal lengths of 30 mm and 65 mm, respectively. The spot radius of the pump light imaged on the laser crystal is approximately 450  $\mu\text{m}$ , which is slightly larger than the laser mode radius at the position of Nd:YVO<sub>4</sub> crystal for improving the beam quality of the laser [26, 27]. Based on the discussion in section 2, a figure “8” shaped ring resonator is employed to ensure the single frequency operation of the laser, and the distance  $d$  is adjusted to 104 mm to obtain stable, high-power laser outputs. The design not only mitigates the thermal effect of the laser crystal to a large extent but also makes the laser to be operated inside the stable range of the resonator at both cases before and after lasing. In the experimental process, we adjusted the distance  $d$  around 104 mm. We found that the stability of the single-frequency laser at 671 nm became worse when the distance  $d < 104$  mm, which confirmed the theoretical analyses in Sec.2.

The gain medium of the laser is a composite Nd:YVO<sub>4</sub> crystal of  $3 \times 3$  mm<sup>2</sup>–cross section and 15-mm length (including an undoped end cap of 5 mm, Nd-doped part of 15 mm with Nd concentration of 0.3%), which is antireflection coated at the pumping wavelength of 880 nm and oscillating wavelength of 1342 nm, and high transmission at 1064 nm to suppress the strong parasitical oscillation at this transition. The low doping concentration and low absorption at 880 nm are advantageous to the thermal effect mitigation [19, 21, 28]. A wedge shaped

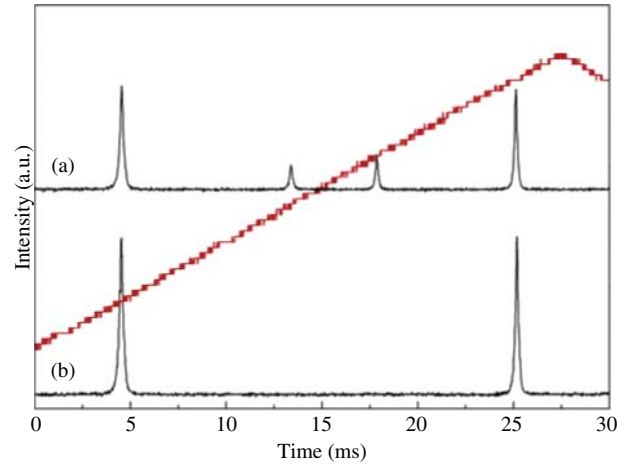


Fig. 4. Scanning confocal Fabry-Perot spectra of the fundamental wave, confirming the single-frequency operation (a) without intracavity nonlinear process and (b) with intracavity nonlinear process. The scanning ramp voltage is also shown.

Nd:YVO<sub>4</sub> crystal with 1.5 degree on its end-facet is used to suppress the oscillation of the unwanted polarization mode [10]. Due to the anisotropy of the Nd:YVO<sub>4</sub> crystal, there exists the thermal lens astigmatism in the laser crystal. In order to eliminate the influence of the thermal lens astigmatism, the Nd:YVO<sub>4</sub> crystal is placed in the laser resonator at a special orientation to make its c-axis in the tangential plane of the laser resonator. In this case, the two different kinds of astigmatisms introduced by the ring cavity and the thermal lens are mutual-compensated. A LBO crystal cut for type-I critical phase matching in the principle plane XZ ( $\theta = 86.1^\circ$ ,  $\phi = 0^\circ$  with  $d_{\text{eff}} = 0.82$  pm/V) is chosen as the nonlinear crystal for frequency doubling due to its high anti-damage threshold and small walk-off angle [13]. The size of the LBO crystal is  $3 \times 3 \times 23$  mm<sup>3</sup> and both end faces are coated with antireflective film at both 1342 nm and 671 nm. The LBO crystal is placed at the position of the beam waist of the ring resonator between M<sub>3</sub> and M<sub>4</sub>. The mirror M<sub>4</sub> is coated with a 0.5% transmission at 1342 nm for obtaining dual wavelength outputs, which is mounted on a translator for adjusting the distance  $d$  between M<sub>3</sub> and M<sub>4</sub> precisely to achieve the optimal single-frequency output at 671 nm. Unidirectional oscillation is ensured by a combination of a Faraday rotator and a zeroth-order half-wave plate (HWP). The Faraday rotator is a cylindrical terbium gallium garnet (TGG) rod placed inside a permanent magnet with a magnetic field of 0.6T to generate about 10-degree polarization rotation for the 1342nm wave. The differential loss between the counterrotating waves is 0.94, which is enough to ensure the unidirectional operation.

### IV. EXPERIMENTAL RESULTS

Before investigating the performance of the intracavity frequency-doubling laser, we optimized the fundamental wave output power by using an output coupler with a transmission of 8% at 1342 nm. The maximum output power of 5.8 W is obtained under the pump power of 23.5 W. When we analyzed the longitudinal-mode construction of the output

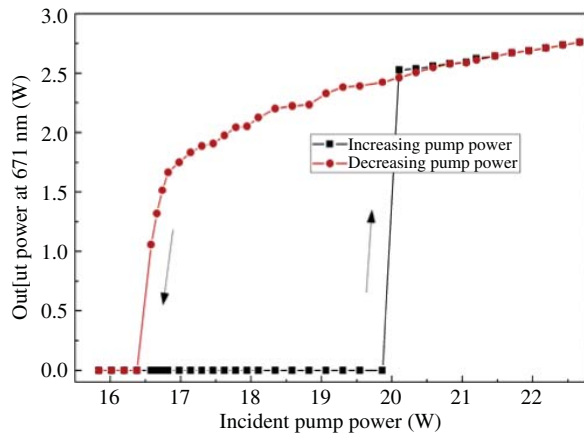


Fig. 5. Output power of the harmonic wave versus incident pump power for increasing and decreasing pump power.

fundamental wave by scanning a confocal Fabry–Perot (F–P) cavity, we found that the single-frequency operation of the laser can only remain for a few seconds and then the mode hop or multi-longitudinal mode operation occurred, as shown in Fig. 4. However, when the output coupler  $M_4$  was replaced with a high-reflective mirror ( $R = 99.5\%$  at 1342 nm) and a LBO crystal was inserted in the resonator, the stable single-frequency operation at 671 nm with the output power of 2.8 W is achieved without the need of an intracavity frequency selector (etalon). The single-frequency operation of 671 nm output is shown in Fig. 4(b). The physical mechanism of the frequency-doubler resulting in single-frequency operation is that the nonlinear process introduces higher loss for neighboring axial modes than that for the main oscillating mode, which suppresses their oscillating [29]. The single-frequency operation at the power level of 2.8 W for three hours was observed. To ascertain the role of the nonlinear mechanism, we changed the temperature of the LBO crystal to 60 °C, which is far away from the phase-matching condition, thus the output of the laser at 671 nm became very weak (only  $\sim 2$  mW), it means that the influence of nonlinear interaction can be ignored. In this case, we found the longitudinal mode became worse again just like that without the doubler (Fig. 4(a)).

When the temperature of LBO was tuned to 27.3 °C (the phase-matching temperature), the maximum single-frequency output power at 671 nm was recorded. Fig. 5 shows the functions of the output powers of the harmonic wave versus the pump powers. Under the pump power of 23.5 W, the second-harmonic output power at 671 nm is 2.8 W, and the fundamental leakage through the output coupler is 850 mW. The laser shows different power characteristic curves for two cases of increasing and decreasing pump powers. Its threshold power is 20 W for the case of increasing pump power, whereas the laser stops working at the pump power of 16.5 W for the case of decreasing pump power. The bistability-like phenomenon mainly results from the distinct difference of the thermal load of the laser at 1342 nm in the two cases of lasing and nonlasing. From Fig. 2, we can see that the laser can oscillate only when the  $f_{th}$  is at the range between 100 mm

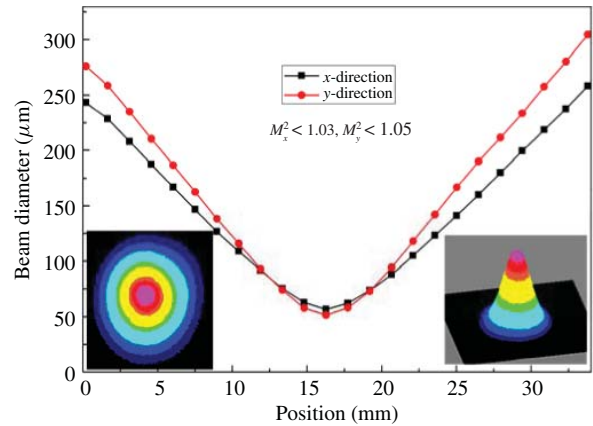


Fig. 6. Measurement of beam quality, spatial beam profile, and intensity distribution.

and 300 mm. The higher the pump power is, the shorter the  $f_{th}$  is. During the process of increasing pump power, the thermal load of the laser crystal increases gradually, the  $f_{th}$  shortens gradually. In the case of nonlasing, the fractional thermal load  $\zeta_0$  is lower ( $\sim 22.5\%$ ), so the  $f_{th}$  is longer than 300 mm before the pump power reaches to 20 W. Until the pump power is more than 20 W, the laser starts to oscillate at 1342 nm, accompanying a step change of thermal load which makes  $f_{th}$  jump from 300 mm to 160 mm due to the higher thermal load of lasing. Increasing the pump power further, the laser kept running smoothly until  $f_{th} < 100$  mm. However, during the process of decreasing the pump power from the lasing state, due to the larger fractional thermal load  $\zeta_0$  ( $\sim 41\%$  of the the 1342 nm lasing a lower pump power of 16.5 W is enough to keep  $f_{th} < 300$  mm. The  $f_{th}$  becomes more than 300 mm after a lower power level of 16.5 W, the laser stops oscillation. The demonstrated experimental results prove the conclusion that the  $\zeta_0$  at 1342 nm lasing is more severe than that without lasing.

Fig. 6 shows the beam diameter of the 671 nm laser versus the distance from the beam waist. Each point is measured by a  $M^2$ meter (DataRay, Inc). From these measured values we can calculate that  $M_x^2$  ( $M_y^2$ ) is 1.03 (1.05). Also, the corresponding spatial beam profile and intensity distribution are also inserted in Fig. 6. The results show that the laser is operating in the  $TEM_{00}$ -mode. By increasing the pump power further, the beam quality of the output beam deteriorates.

## V. CONCLUSION

We have designed and constructed a watt-level single-frequency Nd:YVO<sub>4</sub>/LBO laser with dual wavelength outputs at 671 nm and 1342 nm in which a “figure-8-shaped” ring cavity is utilized. According to the unusually thermal characteristics of Nd:YVO<sub>4</sub> crystal at 1342 nm, we analyze the oscillating condition of 1342 nm lasing, to ensure that the laser stability condition can be satisfied at both cases before and after lasing. Based on the analysis results, the cavity parameters are optimized to mitigate the thermal effect of gain medium. The stability of the single-longitudinal-mode operation at both cases with and without nonlinear conver-

sion is compared, and the stable operation of the frequency-doubling single-frequency laser at 671 nm is achieved. The maximal single-frequency output power of 2.8 W at 671 nm, and the fundamental leakage power of 850 mW at 1342 nm through the output coupler are obtained simultaneously. The mode-hop-free single-frequency operation of more than 3 h is observed. The single-frequency lasers at the two wavelengths can be used for the pump field, and the injected signal of an OPA to produce the entangled optical fields, which have potential application in developing quantum information networks [7, 30].

## REFERENCES

- [1] A. Di Lieto, P. Minguzzi, A. Pirastu, S. Sanguinetti, and V. Magni, "A 7-W diode-pumped Nd:YVO<sub>4</sub> CW laser at 1.34  $\mu\text{m}$ ," *Appl. Phys. B*, vol. 75, nos. 4–5, pp. 463–466, 2002.
- [2] A. Di Lieto, P. Minguzzi, A. Pirastu, S. Sanguinetti, A. Toncelli, and V. Magni, "High-power diffraction-limited diode-pumped Nd:YVO<sub>4</sub> CW laser at 1.3  $\mu\text{m}$ ," *Adv. Solid-State Lasers*, vol. 68, pp. 570–574, Feb. 2002.
- [3] I. E. Olivares, A. E. Duarte, E. A. Saravia, and F. J. Duarte, "Lithium isotope separation with tunable diode lasers," *Appl. Opt.*, vol. 41, no. 15, pp. 2973–2977, 2002.
- [4] N. B. Grosse, W. P. Bowen, K. Mckenzie, and P. L. Lam, "Harmonic entanglement with second-order nonlinearity," *Phys. Rev. Lett.*, vol. 96, no. 6, pp. 063601-1–063601-4, Feb. 2006.
- [5] R. G. Yang, S. Q. Zhai, K. Liu, J. X. Zhang, and J. R. Gao, "Generation of multicolored tripartite entanglement by frequency doubling in a two-port resonator," *J. Opt. Soc. Amer. B*, vol. 27, no. 12, pp. 2721–2726, 2010.
- [6] L. J. Radziemski, R. Engleman, and J. W. Brault, "Fourier-transform-spectroscopy measurements in the spectra of neutral lithium, <sup>6</sup>Li I and <sup>7</sup>Li I (Li I)" *Phys. Rev. A*, vol. 52, no. 6, pp. 4462–4470, 1995.
- [7] H. J. Kimble, "The quantum internet," *Nature*, vol. 453, pp. 1023–1030, Jun. 2008.
- [8] H. Ogilvy, M. J. Withford, P. Dekker, and J. A. Piper, "Efficient diode double-end-pumped Nd:YVO<sub>4</sub> laser operating at 1342 nm," *Opt. Exp.*, vol. 11, no. 19, pp. 2411–2415, 2003.
- [9] A. Y. Yao, W. Hou, Y. Bi, A. C. Geng, X. C. Lin, Y. P. Kong, D. F. Cui, L. A. Wu, and Z. Y. Xu, "High-power CW 671 nm output by intracavity frequency doubling of a double-end-pumped Nd:YVO<sub>4</sub> laser," *Appl. Opt.*, vol. 44, no. 33, pp. 7156–7160, 2005.
- [10] F. Lenhardt, A. Nebel, R. Knappe, M. Nittmann, J. Bartschke, and J. A. Lhuillier, "Efficient single-pass second harmonic generation of a continuous wave Nd:YVO<sub>4</sub> - laser at 1342 nm using MgO:PPLN," in *Proc. Conf. Lasers Electro-Opt.*, May 2010, no. CThEE5, pp. 1–2.
- [11] A. Agnesi, G. C. Reali, and P. G. Gobbi, "430-mW single-transverse mode diode-pumped Nd:YVO<sub>4</sub> laser at 671 nm," *IEEE J. Quantum Electron.*, vol. 34, no. 7, pp. 1297–1300, Jul. 1998.
- [12] Y. H. Zheng, F. Q. Li, Y. J. Wang, K. S. Zhang, and K. C. Peng, "High-stability single-frequency green laser with a wedge Nd:YVO<sub>4</sub> as a polarizing beam splitter," *Opt. Commun.*, vol. 283, no. 2, pp. 309–312, Jan. 2010.
- [13] F. A. Camargo, T. Z. Willette, T. Badr, N. U. Wetter, and J. J. Zondy, "Tunable single-frequency Nd:YVO<sub>4</sub>/BiB<sub>3</sub>O<sub>6</sub> ring laser at 671 nm," *IEEE J. Quantum Electron.*, vol. 46, no. 5, pp. 804–809, May 2010.
- [14] M. Okida, M. Itoh, T. Yatagai, H. Ogilvy, J. Piper, and T. Omatsu, "Heat generation in Nd doped vanadate crystals with 1.34  $\mu\text{m}$  laser action," *Opt. Exp.*, vol. 13, no. 13, pp. 4909–4915, 2005.
- [15] L. Fornasiero, T. Kellner, S. Kück, J. P. Meyn, P. E. A. Möbert, and G. Huber, "Excited state absorption and stimulated emission of Nd<sup>3+</sup> in crystals III: LaSc<sub>3</sub>(BO<sub>3</sub>)<sub>4</sub>, CaWO<sub>4</sub>, and YLiF<sub>4</sub>," *Appl. Phys. B*, vol. 68, no. 1, pp. 67–72, 1998.
- [16] F. Lenhardt, M. Nittmann, T. Bauer, J. Bartschke, and J. A. Lhuillier, "High-power 888-nm-pumped Nd:YVO<sub>4</sub> 1342-nm oscillator operating in the TEM<sub>00</sub> mode," *Appl. Phys. B*, vol. 96, no. 4, pp. 803–807, 2009.
- [17] X. Ding, R. Wang, H. Zhang, X. Y. Yu, W. Q. Wen, P. Wang, and J. Q. Yao, "High-efficiency Nd:YVO<sub>4</sub> laser emission under direct pumping at 880 nm," *Opt. Commun.*, vol. 282, no. 5, pp. 981–984, 2009.
- [18] Y. F. Lv, X. H. Zhang, J. Xia, X. D. Yin, A. F. Zhang, L. Bao, and W. Lv, "High-efficiency direct-pumped Nd:YVO<sub>4</sub>-LBO laser operating at 671 nm," *Opt. Laser Technol.*, vol. 42, no. 3, pp. 522–525, Apr. 2010.
- [19] L. McDonagh and R. Wallenstein, "Low-noise 62 W CW intracavity-doubled TEM<sub>00</sub> Nd:YVO<sub>4</sub> green laser pumped at 888 nm," *Opt. Lett.*, vol. 32, no. 7, pp. 802–804, 2007.
- [20] M. E. Innocenzi, H. T. Yura, C. L. Fincher, and R. A. Fields, "Thermal modeling of continuous-wave end-pumped solid-state lasers," *Appl. Phys. Lett.*, vol. 56, no. 19, pp. 1831–1833, May 1990.
- [21] W. A. Clarkson, "Thermal effects and their mitigation in end-pumped solid-state lasers," *J. Phys. D: Appl. Phys.*, vol. 34, no. 16, pp. 2381–2395, 2001.
- [22] Y. F. Chen, Y. P. Lan, and S. C. Wang, "Influence of energy-transfer upconversion on the performance of high-power diode-end-pumped CW lasers," *IEEE J. Quantum Electron.*, vol. 36, no. 5, pp. 615–619, May 2000.
- [23] P. J. Hardman, W. A. Clarkson, G. J. Friel, M. Pollnau, and D. C. Hanna, "Energy-transfer upconversion and thermal lensing in high-power end-pumped Nd:YLF laser crystals," *IEEE J. Quantum Electron.*, vol. 35, no. 4, pp. 647–655, Apr. 1999.
- [24] Y. J. Wang, Y. H. Zheng, C. D. Xie, and K. C. Peng, "High-power low-noise Nd:YAP/LBO laser with dual wavelength outputs," *IEEE J. Quantum Electron.*, vol. 47, no. 7, pp. 1006–1013, Jul. 2011.
- [25] W. J. Xie, S. C. Tam, Y. L. Lam, H. R. Yang, J. H. Gu, G. Zhao, and W. Tan, "Influence of pump beam size on laser diode end-pumped solid state lasers," *Opt. Laser Technol.*, vol. 31, no. 8, pp. 555–558, Nov. 1999.
- [26] X. Y. Peng, L. Xu, and A. Asundi, "Power scaling of diode-pumped Nd:YVO<sub>4</sub> lasers," *IEEE J. Quantum Electron.*, vol. 38, no. 9, pp. 1291–1299, Sep. 2002.
- [27] N. Pavel, C. Krankel, R. Peters, K. Petermann, and G. Huber, "In-band pumping of Nd-vanadate thin-disk lasers," *Appl. Phys. B*, vol. 91, nos. 3–4, pp. 415–419, 2008.
- [28] E. Cheng, D. R. Dudley, W. L. Nighan, J. D. Kafka, D. E. Spence, and D. S. Bell, "Lasers with low doped gain medium," U.S. Patent 6 185 235, Feb. 6, 2001.
- [29] K. I. Martin, W. A. Clarkson, and D. C. Hanna, "Self-suppression of axial mode hopping by intracavity second-harmonic generation," *Opt. Lett.*, vol. 22, no. 6, pp. 375–377, 1997.
- [30] W. Yao, R. B. Liu, and L. J. Sham, "Theory of control of the spin-photon interface for quantum networks," *Phys. Rev. Lett.*, vol. 95, no. 3, pp. 030504-1–030504-4, Jul. 2005.



**Yaohui Zheng** was born in 1979. He received the M.S. degree in optical engineering and the Ph.D. degree in laser technology from Shanxi University, Shanxi, China, in 2004 and 2009, respectively.

He is currently a Researcher with the Institute of Opto-Electronics, Shanxi University. His current research interests include high-power single-frequency lasers, quantum optics devices, and nonlinear optics.



**Yajun Wang** received the B.S. degree in physics from Shanxi University, Shanxi, China, in 2008. He is currently pursuing the Ph.D. degree in all-solid-state single-frequency lasers with the Institute of Opto-Electronics, Shanxi University.

His current research interests include single-frequency lasers and nonlinear optics.



**Changde Xie** was born in 1939. She received the B.S. degree in physics from Sichuan University, Chengdu, China, in 1961.

She was a Visiting Scholar with the University of Texas, Austin, from 1982 to 1984 and 1988 to 1989. Since 1990, she has been a Professor with the Institute of Opto-Electronics, Shanxi University, Shanxi, China. Her current research interests include quantum computers, quantum information networks, and quantum optics devices.

Prof. Xie was elected as a fellow of the Optical Society of America in April 2009 and is a member of the Chinese Physical Society.



**Kunchi Peng** was born in 1936. He received the B.S. degree in physics from Sichuan University, Chengdu, China, in 1961.

He was a Visiting Scholar with Paris' 11th University, Orsay, France, the University of Texas, Austin, and the California Institute of Technology, Pasadena, from 1980 to 1982, 1982 to 1984, and 1988 to 1989, respectively. He has been a Professor with the Institute of Opto-Electronics, Shanxi University, Shanxi, China, since 1990. His current research interests include all-solid-state laser technology, quantum information networks, and quantum optics devices.

Prof. Peng was elected as a fellow of the Optical Society of America in April 2006 and is a member of the Chinese Physical Society.